Multivariable sliding mode approach with enhanced robustness properties based on the robust internal-loop compensator for a class of nonlinear mechanical systems

Almir Salihbegovic[1]

Abstract— **This paper proposes the synthesis of the integral sliding mode control (I-SMC) and the robust internal-loop compensator (RIC) for nonlinear multiple-input multiple-output (MIMO) systems, introducing a generalization of the well-known single-input single-output (SISO) case for linear systems. The new control term is introduced in order to incorporate a RIC structure with a multivariable I-SMC scheme for a class of nonlinear mechanical systems affected by perturbations. The finite-time stability of the closed-loop system is discussed using a Lyapunov based approach. The designed algorithm is used to control attitudes of the small-scale laboratory helicopter system, representing a nonlinear MIMO system with significant cross-couplings and inherently unstable characteristics. An excellent tracking performance and robustness properties of the proposed control method is demonstrated through both, computer simulation and experimental testing, even in the presence of additional internal and external disturbances.**

I. Introduction

There are two major requirements in the design procedure of a robust control for a system in the presence of uncertainties and disturbances: performance specifications of the closed-loop system and robustness properties to the modeling uncertainties, external disturbances and physical parameter variations. Sliding mode control has been popular technique for robust control over many decades due to its invariance to the matching uncertainties [1]. One of the main disadvantages of the traditional SMC is the chattering effect due to the discontinuous control [1]. Successful employments of the multivariable sliding mode approach have opened the door for its integration with other techniques for disturbance compensation and chattering reduction [2]–[6]. In order to achieve quantified trade-off between performance specifications and robustness properties, a generalized disturbance attenuation framework called robust internal-loop compensator (RIC) is proposed [7]–[11]. It is shown that the RIC structure ensures unified analysis of the model based disturbance attenuation algorithms such as adaptive robust control [8], disturbance observer [9] and sliding mode control [11]. Although effective performances have been demonstrated, the concepts of the RIC are presented only for a class of linear single-input single-output (SISO) systems.

This paper presents an extension of the RIC method for linear SISO systems, introduced in [7]–[11], to a class of nonlinear MIMO systems affected with perturbations. The synthesis of the multivariable I-SMC and the RIC is proposed through the Lyapunov redesign framework by using the new control term, that enhances robust stability of the closed-loop system, attenuates chattering phenomenon of the sliding modes and provide systematic performance tuning. In addition to the disturbance observer (DOB) based SMC schemes [12], [13], this paper discusses uniformly ultimately boundedness of the closed-loop system solutions, thus achieving enhanced robustness to the disturbance compensation error.

The effectiveness of the developed control structure is evaluated to the small-scale laboratory helicopter system CE 150 supplied by Humosoft, which represents a highly nonlinear MIMO system with significant cross-couplings and modeling uncertainties. Therefore, various control techniques [14], [15] have already been tested on the laboratory helicopter system CE 150, such as: linear quadratic optimal control combined with a state estimator (LQG), fuzzy based control, model predictive control (MPC), etc. However, presented results did not demonstrate effective compensation of cross-coupling effects, parametric uncertainties and external disturbances, thus tracking performances and robust stability of the helicopter CE 150 are slightly degraded. Significant reduction of the power consumption and improvement of the helicopter tracking performances are achieved using the linear disturbance observers [12]. In [13] DOB based SMC method for the helicopter system CE 150 is evaluated in the presence of additional external disturbances and parametric uncertainties, and enhanced performance specifications are presented. In this work, we expose the helicopter system to the influence of wind gusts and 30% uncertainties on the model parameters are applied as in [13] to verify the robustness of the proposed control algorithm. In addition to the previous papers [12]–[15], the additional control input of the helicopter is employed here, which allows motion of the small ballast along its horizontal axis, thus dynamic changes in the center of gravity are simulated. Excellent tracking performances will be shown through both, computer simulation and experimental testing, even in the presence of these external disturbances and parametric uncertainties.

The paper is organized as follows. The synthesis of the I-SMC and the RIC for a class of nonlinear MIMO uncertain systems is presented in Section II. Implementation of the developed control algorithm to the laboratory helicopter model CE 150 is presented in Section III. Simulation and experimental results are discussed in Section IV. Concluding remarks are given in Section V.

[1]Almir Salihbegovic is with Faculty of Electrical Engineering, Department for Automatic Control and Electronics, University of Sarajevo, 71000 Sarajevo, Bosnia and Herzegovina almir.salihbegovic@etf.unsa.ba

II. Multivariable I-SMC based on the RIC

This section presents the synthesis of the I-SMC scheme and the RIC for a class of nonlinear MIMO systems with parametric uncertainties and external disturbances.

Consider a MIMO nonlinear mechanical system (either translational or rotational) [16]:

$$a(q)\ddot{q}(t) + b(q,\dot{q}) + \tau_d\left(t,q,\dot{q},\tau\right) = \tau\left(t,q,\dot{q}\right), \quad (1)$$

where $q(t) \in \mathbb{R}^n$ and $\dot{q}(t) \in \mathbb{R}^n$ represent the state vectors, position and velocity, respectively, $\tau\left(t,q,\dot{q}\right) \in \mathbb{R}^n$ is the control input vector, $a(q) \in \mathbb{R}^{n\times n}$ is the nonsingular matrix denoting inertia of the system, $b(q,\dot{q}) \in \mathbb{R}^n$ is the nonlinear vector representing Coriolis and friction torques, and $\tau_d(t,q,\dot{q},\tau)$ stands for the plant input disturbance vector that includes gravitational torque and external disturbances. The functions $a(q)$, $b(q,\dot{q})$ and $\tau_d(t,q,\dot{q},\tau)$ are defined for $(t,q,\dot{q},\tau) \in [0,\infty) \times D \times D \times D$, where $D \subset \mathbb{R}^n$ is a domain that contains the origin. Assume that $a(q)$, $b(q,\dot{q})$ and $\tau_d\left(t,q,\dot{q},\tau\right)$ are sufficiently smooth functions in terms of state variables q and $\dot{q}$, so that with the feedback control $\tau = \tau(t,q,\dot{q})$, that is sufficiently smooth control vector, the closed-loop system will have a unique solution through every point $(t_0,q_0,\dot{q}_0) \in [0,\infty)\times D\times D$. The acceleration $\ddot{q}(t)$ and the state variables $q(t)$ and $\dot{q}(t)$ are also assumed continuous and bounded. The perturbed system can be described with:

$$a_n\ddot{q}(t) + b_n\dot{q}(t) + \tau_{dis}\left(t,q,\dot{q},\tau\right) = \tau\left(t,q,\dot{q}\right), \quad (2)$$

where a_n is the $n\times n$ matrix of nominal inertia coefficients, b_n is the $n \times n$ matrix of nominal friction coefficients, $\tau_{dis} = \tau_d + \Delta a(q)\ddot{q} + \Delta b(q,\dot{q})\dot{q}$ denotes the generalized disturbance vector that may include various uncertain terms caused by model simplification and parametric uncertainties, $\Delta a(q)\ddot{q}$ and $\Delta b(q,\dot{q})\ddot{q}$ represent the torque vectors induced by varying inertia matrix $\Delta a(q) = a(q) - a_n$ and varying friction matrix $\Delta b(q,\dot{q}) = b(q,\dot{q}) - b_n$, respectively. The tracking error vector $e(t,q)$ defines the difference between the output vector $q(t)$ and the reference vector $q_{ref}(t)$:

$$e(t,q) = q(t) - q_{ref}(t), \quad (3)$$

where $q_{ref}(t)$ is sufficiently smooth vector function. In equilibrium, the output vector $q(t)$ of the system should be constrained to the manifold [16]:

$$S_1 = \left\{ q \middle|\, e(t,q) = 0 \right\}. \quad (4)$$

The generalized error vector $\sigma\left(t,q,\dot{q}\right) \in \mathbb{R}^n$ is introduced in order to provide relative degree one ($r = 1$) with respect to the control vector τ:

$$\sigma\left(t,q,\dot{q}\right) = \dot{e}(t,q) + \Lambda_1 e(t,q) + \Lambda \int_0^t e(t,q)\,\mathrm{d}t, \quad (5)$$

where Λ_1 and Λ are $n\times n$ positive constant matrices. The integral tracking error vector is included in the generalized error vector (5) to reduce the steady state error. Now, the goal is to drive the outputs of the system to the integral sliding manifold:

$$S_2 = \left\{ q \middle|\, \sigma(t,q,\dot{q}) = 0 \right\}. \quad (6)$$

First, we design a stabilizing controller using the nominal model of the system (2):

$$a_n\ddot{q}_n(t) + b_n\dot{q}_n(t) = \tau_n\left(t,q,\dot{q}\right), \quad (7)$$

where $q_n(t)$ is the nominal output vector generated internally by the nominal control vector $\tau_n\left(t,q,\dot{q}\right)$. The generalized error dynamics for the nominal system is calculated using (5) and (7):

$$\dot{\sigma} = a_n^{-1}\tau_n - \left(\ddot{q}_{ref} + \Lambda_1\dot{q}_{ref} - \Lambda e\right), \quad (8)$$

where $\Lambda_1 = a_n^{-1}b_n$. The equivalent control vector is selected to cancel right-hand side of (8) [17]:

$$\tau_{eq} = a_n\ddot{q}_{ref} + b_n\dot{q}_{ref} - a_n\Lambda e. \quad (9)$$

Next, for the actual system (2) affected by disturbances τ_{dis} we design the overall control τ as follows:

$$\tau\left(t,q,\dot{q}\right) = \tau_{eq}\left(t,q,\dot{q}\right) + \hat{\tau}_{dis}\left(t,q,\dot{q}\right) + \tau_v\left(t,q,\dot{q}\right). \quad (10)$$

Here, feedback control vectors $\hat{\tau}_{dis}(t,q,\dot{q})$ and $\tau_v(t,q,\dot{q})$ need to be designed so that the overall control (10) stabilizes the resulting closed-loop system:

$$a_n\ddot{q} + b_n\dot{q} = \tau_{eq} + \tau_v + \hat{\tau}_{dis} - \tau_{dis}, \quad (11)$$

in the presence of parametric uncertainties and external disturbances. The additional control vector $\hat{\tau}_{dis}$ is included in the overall control (10) in order to estimate generalized disturbances τ_{dis} and attenuate chattering phenomenon by reducing the magnitudes of the sliding mode control. The additional control vector τ_v is introduced to force sliding mode motion toward the manifold (6) and attenuation of the disturbance compensation error vector:

$$p\left(\tau_{dis},\hat{\tau}_{dis}\right) = \tau_{dis} - \hat{\tau}_{dis}. \quad (12)$$

The disturbance estimation error vector $p\left(\tau_{dis},\hat{\tau}_{dis}\right)$ can be treated as the input disturbance vector in the closed-loop system (11). Thus, the switching gains of the additional control vector τ_v are only required to be grater than the magnitudes of the disturbance compensation error vector p, rather then that of the whole generalized disturbance vector τ_{dis}.

For the system (11), consider a Lyapunov function candidate:

$$V = \frac{\sigma^T\sigma}{2},\ V(0) = 0. \quad (13)$$

The first order time derivative $\dot{V} = \sigma^T\dot{\sigma}$ depends on the generalized error dynamics of the perturbed system (11):

$$\dot{\sigma} = a_n^{-1}\left(\tau_v + \hat{\tau}_{dis} - \tau_{dis}\right). \quad (14)$$

The function $\dot{V}$ along the trajectories of the system (11) is calculated using (14):

$$\dot{V} = a_n^{-1}\sigma^T(\tau_v + \hat{\tau}_{dis} - \tau_{dis}) \quad (15)$$

$$= a_n^{-1}\sigma^T(\tau_v - p). \quad (16)$$

Hence, if $\hat{\tau}_{dis}$ is arranged to attenuate the generalized disturbance vector τ_{dis}, the additional control vector τ_v could be managed to cancel the effect of the disturbance estimation

error p on $\dot{V}$ in (16), so that $a_n^{-1}\sigma^T(\tau_v - p) \leq -a_n^{-1}\eta_{20}\|\sigma\|_1$ is satisfied, where η_{20} is a positive constant.

Suppose that with the control (10), the generalized disturbance vector τ_{dis} satisfies the inequality [17]:

$$0 \leq \|\tau_{dis}\|_\infty \leq \rho(t, q, \dot{q}) + k_1\|\hat{\tau}_{dis}\|_\infty + k_2\|\tau_v\|_\infty, \quad (17)$$

where $\rho : [0, \infty) \times D \times D \to \mathbb{R}$ is a nonnegative continuous function representing a measure of the size of disturbances, $k_1 \in [-1, 0]$ and $k_2 \in [0, 1)$ are scalar constants. The estimate (17) is the only information we should know about the generalized disturbances τ_{dis}. We do not require for the function ρ to be small, but only to be known. The control objective is to show that with the knowledge of V, ρ, k_1 and k_2, we can design additional control vectors $\hat{\tau}_{dis}$ and τ_v, so that the overall control (10) will stabilize the actual system (11) in the presence of parametric uncertainties and external disturbances.

Applying the Cauchy-Schwarz inequality $\left|\sigma^T\tau_{dis}\right| \leq \|\sigma\|_1\|\tau_{dis}\|_\infty$ and the upper bound of (17) to the most right product term of (15), it follows:

$$\begin{aligned}\dot{V} \leq\ & a_n^{-1}\left(\sigma^T\hat{\tau}_{dis} + k_1\|\sigma\|_1\|\hat{\tau}_{dis}\|_\infty\right) \\ & + a_n^{-1}\left(\sigma^T\tau_v + k_2\|\sigma\|_1\|\tau_v\|_\infty + \rho\|\sigma\|_1\right). \quad (18)\end{aligned}$$

We use the traditional sliding control vector τ_v [17]:

$$\tau_v = -\frac{1}{1-k_2}\eta_2 \cdot \mathrm{sgn}(\sigma), \quad (19)$$

and propose new control vector $\hat{\tau}_{dis}$ for disturbance attenuation based on the RIC:

$$\hat{\tau}_{dis} = -\frac{1}{1-k_1}(\eta_1 * \sigma). \quad (20)$$

Here $\eta_1 = \mathrm{diag}(\eta_{11}, \ldots, \eta_{1n})$ is a $n \times n$ matrix with nonnegative functions $\eta_{1i}(t)$, $\forall t \in [0, \infty)$. $\eta_2(t, q, \dot{q})$ is nonegative scalar function $\forall (t, q, \dot{q}) \in [0, \infty) \times D \times D$, $\mathrm{sgn}(\sigma) = \left[\mathrm{sgn}(\sigma_1), \ldots, \mathrm{sgn}(\sigma_n)\right]^T$ is a vector of signs of sliding surfaces and $\eta_1 * \sigma = [\eta_{11} * \sigma_1, \ldots, \eta_{1n} * \sigma_n]^T$ represents a vector of convolutions of η_{1i} and σ_i, for all $i = 1, \ldots, n$. Applying the control vectors (19) and (20) to (18), it yields:

$$\begin{aligned}\dot{V} \leq\ & a_n^{-1}\left[\frac{k_1}{1-k_1}\|\sigma\|_1\|\eta_1 * \sigma\|_\infty - \frac{1}{1-k_1}\sigma^T(\eta_1 * \sigma)\right] \\ & + a_n^{-1}\left[\frac{k_2}{1-k_2}\eta_2\|\sigma\|_1 - \frac{1}{1-k_2}\eta_2\|\sigma\|_1 + \rho\|\sigma\|_1\right]. \quad (21)\end{aligned}$$

The scalar function $\sigma^T(\eta_1 * \sigma)$ on the right-hand side of (21) is nonnegative, namely $\sigma^T(\eta_1 * \sigma) = \left|\sigma^T(\eta_1 * \sigma)\right|$, since $\sigma_i(\eta_{1i} * \sigma_i)$ are nonnegative functions for all $\eta_{1i} \geq 0$ and $i = 1, \ldots, n$. The bounds of the scalar function $\left|\sigma^T(\eta_1 * \sigma)\right|$ could be derived using the Cauchy-Schwarz inequality and the Young's inequality for convolution:

$$\left|\sigma^T(\eta_1 * \sigma)\right| \leq \|\sigma\|_1\|\eta_1 * \sigma\|_\infty \leq \|\eta_1\|_\infty\|\sigma\|_1^2. \quad (22)$$

The lower bound of (22) is selected as:

$$(\rho - p_0)\|\sigma\|_1 \leq \left|\sigma^T(\eta_1 * \sigma)\right|, \quad (23)$$

where p_0 is a positive constant representing bounds of the disturbance estimation error vector, namely $\|p\|_\infty \leq p_0$ and $\rho > p_0$. Here, the bounds (22) and (23) are selected such that the function $\dot{V}$ is negative definite outside the set Ω_η:

$$\Omega_\eta = \left\{\|\sigma\|_1 \leq \frac{\rho - p_0}{\|\eta_1\|_\infty}\right\}. \quad (24)$$

Using (21), (22) and (23), it follows:

$$\begin{aligned}\dot{V} &\leq a_n^{-1}\left(-\left|\sigma^T(\eta_1 * \sigma)\right| - \eta_2\|\sigma\|_1 + \rho\|\sigma\|_1\right) \quad (25)\\ &\leq -a_n^{-1}\eta_{20}\|\sigma\|_1 = -a_n^{-1}\eta_{20}\sqrt{2V}, \quad (26)\end{aligned}$$

where η_{20} is positive constant such that $\eta_{20} \leq \eta_2 - p_0$. Hence, the function $\dot{V}$ is negative definite along the trajectories of the closed-loop system (11) if the inequalities:

$$\|\eta_1\|_\infty \geq \frac{\rho - p_0}{\|\sigma\|_1}, \quad (27)$$

$$\eta_2 \geq p_0 + \eta_{20}, \quad (28)$$

hold. The system trajectories reach the positively invariant set (24) in finite time and remain inside thereafter. Therefore, the solutions of the perturbed system (11) are uniformly ultimately bounded. The radius of the boundary layer (24) can be made small enough by increasing the magnitude $\|\eta_1\|_\infty$ in order to drive the system states to an arbitrarily small neighborhood of the origin. The magnitude η_1 of the robust compensator $\hat{\tau}_{dis}$ should be designed so the maximum value of the disturbance estimation error is p_0. Then, the magnitude η_2 of the sliding mode control term τ_v should be selected to dominate over the maximum value of disturbance compensation error p_0, instead of the whole disturbance τ_{dis}. Thus, the magnitude of the switching control term can be decreased in order to reduce the chattering effect.

III. Application to the helicopter system CE 150

The laboratory helicopter system Humosoft CE 150 consists of the rigid body with the ballast, the massive support and two propellers driven by DC motors, the power supply unit and the interface module. The control strategy of the helicopter is not presented here, due to the space limit. Since it is not in focus of this paper, the detailed control strategy is given in our previous papers [12], [13], [18].

A. Helicopter dynamics model

This subsection introduces the mathematical model of the laboratory helicopter system CE 150 with two degrees of freedom: the elevation (pitch) ψ and the azimuth (yaw) φ. It has three inputs (the main motor voltage u_1, the tail motor voltage u_2 and the servomotor voltage u_3 that controls the ballast position along the horizontal bar), and two outputs (elevation and azimuth). The operating ranges of the helicopter input and output variables are given in Tab. I. Since the detailed modeling procedure of the helicopter complete dynamics is not in scope of this paper, only the main results are presented here.

TABLE I: Constraints for the helicopter input and output signals

		Operational range
Inputs	u_1	$[0,\ 0.6]$
	u_2	$[-0.3,\ 0.3]$
	u_3	$[-1,\ 0]$
Outputs	ψ	$[-45°,\ 45°]$
	φ	$[-130°,\ 130°]$

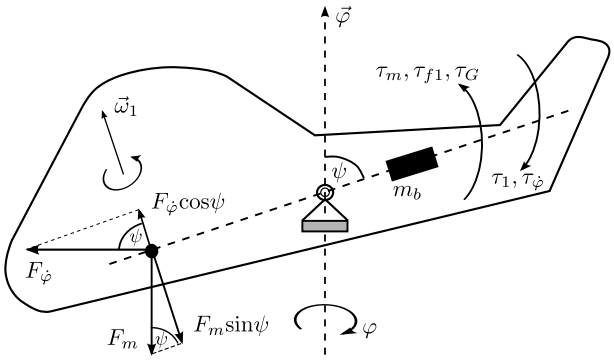

Fig. 1: Torques acting on the helicopter body in the vertical plane

As Fig. 1 shows, the torques balance in the vertical plane is used to describe the elevation dynamics [12], [13], [18]:

$$a_\psi \ddot{\psi} = \tau_1 + \tau_{\dot{\varphi}} - \tau_{f_1} - \tau_m - \tau_G, \tag{29}$$

$$\tau_{\dot{\varphi}} = ml\dot{\varphi}^2 \sin\psi \cos\psi, \tag{30}$$

$$\tau_{f_1} = C_\psi \operatorname{sgn}\dot{\psi} + B_\psi \dot{\psi}, \tag{31}$$

$$\tau_m = mgl \sin\psi, \tag{32}$$

$$\tau_G = K_G \dot{\varphi} \omega_1 \cos\psi, \text{ for } \dot{\varphi} \ll \omega_1. \tag{33}$$

Here, a_ψ stands for a moment of inertia around the horizontal axis, τ_1 is a moment produced by the main propeller, $\tau_{\dot{\varphi}}$ denotes a centrifugal torque, τ_{f_1} represents Coulumb and viscous friction torques, τ_m is a gravitation torque, τ_G stands for a gyroscopic torque, m is the helicopter mass, g denotes the gravitational acceleration, l is the distance from the vertical axis to the main motor axis, ω_1 represents an angular velocity of the main propeller, K_G is the gyroscopic coefficient, B_ψ and C_ψ stand for viscous and Coulumb friction coefficients, respectively. Some influences are neglected in (29)−(33), such as motor stabilizing torque and air resistance variation, which should be compensated by the the elevation disturbance observer.

The azimuth dynamics considers the torques in the horizontal plane, yielding the equations [12], [13], [18]:

$$a_\varphi \ddot{\varphi} = \tau_2 - \tau_{f_2} - \tau_r, \tag{34}$$

$$\tau_{f_2} = C_\varphi \operatorname{sgn}\dot{\varphi} + B_\varphi \dot{\varphi}, \tag{35}$$

$$a_\varphi = a_\psi \sin\psi, \tag{36}$$

where a_φ denotes a moment of inertia around the vertical axis, τ_2 is a moment produced by the tail propeller, τ_{f_2} represents Coulumb and viscous friction torques, τ_r is a reaction torque of the main motor, ω_2 denotes an angular velocity of the tail propeller, B_φ and C_φ stand for viscous and Coulumb friction coefficients. The azimuth disturbance observer should compensate coupling effects between the azimuth friction torque and the tail propeller speed, which are not considered in (34)-(36).

B. The empirical model of the main DC motor and the main propeller dynamics

Due to the helicopter body structure, which does not allow direct physical access to the appropriate internal signals, the main DC motor dynamics is approximated with the second order transfer function [12], [13], [18]:

$$\frac{\omega_1(s)}{u_1(s)} = \frac{1}{(T_1 s + 1)^2}. \tag{37}$$

Here, $\omega_1(s)$ and $u_1(s)$ represent Laplace transforms of $\omega_1(t)$ and $u_1(t)$, respectively, and T_1 is the main motor time constant. The main propeller torque is approximated with the parabolic function of the angular velocity [12], [13], [18]:

$$\tau_1(t) = a_1 \omega_1^2(t) + b_1 \omega_1(t), \tag{38}$$

where a_1 and b_1 are parameters of the main propeller characteristic. Also, analogue relations to (37) and (38) are applicable for the tail DC motor with parameters T_2, a_2 and b_2.

C. The empirical model of the cross-coupling dynamics

The precise identification of the interaction torques is not possible for the helicopter CE 150, since no appropriate signal is available for measurements. Therefore, the main motor reaction torque to the azimuth dynamics is approximated as follows [12], [13], [18]:

$$\frac{\tau_r(s)}{u_1(s)} = K \frac{T_z s + 1}{T_p s + 1}, \tag{39}$$

where T_z and T_p are time constants considered in the identification process. A simple genetic algorithm [14] has been designed to determine all unknown parameters. The values of the helicopter model parameters are presented in [12].

D. Control Design

The helicopter complete dynamics (29)-(39) could be described by (2) introducing substitutes:

$$\tau = \begin{bmatrix} \tau_1 \\ \tau_2 \end{bmatrix},\ \tau_{dis} = \begin{bmatrix} \tau_{f1} + \tau_m + \tau_G - \tau_{\dot{\varphi}} \\ \tau_{f2} + \tau_r \end{bmatrix}. \tag{40}$$

Two disturbance observers of the first order are employed in order to attenuate parametric uncertainties and external disturbances of the helicopter system CE 150:

$$Q(s) = \lambda \cdot \operatorname{diag}\left(\frac{1}{s + \lambda_1}, \frac{1}{s + \lambda_2} \right), \tag{41}$$

where $\lambda = \operatorname{diag}(\lambda_1, \lambda_2)$ is a matrix of constants λ_1 and λ_2, which represent cut-off frequencies of disturbance observers for the elevation and the azimuth dynamics, respectively. Then the robust compensator has the form [7]–[10]:

$$K(s) = a_n \lambda s. \tag{42}$$

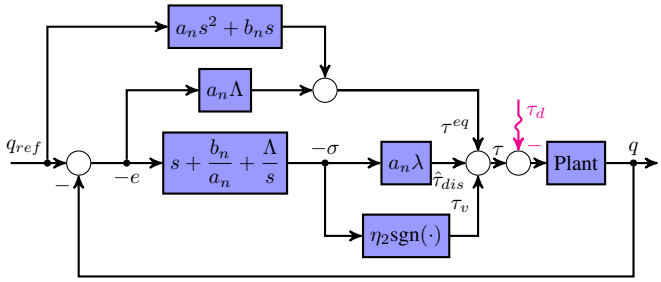

Fig. 2: The proposed RIC-SMC scheme for the nonlinear uncertain MIMO systems

By comparing the Laplace representation of the control input (20) for $k_1 = 0$, that is $\hat{\tau}_{dis}(s) = -\eta_1(s)\sigma(s)$, with the additional control for the disturbance compensation based on the RIC in [7]–[10], it follows:

$$\eta_1(s) = \frac{K(s)}{s}, \tag{43}$$

and the function matrix $\eta_1(t)$ is derived:

$$\eta_1(t) = \mathcal{L}^{-1}\left\{\frac{K(s)}{s}\right\} = a_n\lambda. \tag{44}$$

Now, the control law of the proposed algorithm for the laboratory helicopter system CE 150 is designed as:

$$\tau = a_n\ddot{q}_{ref} + b_n\dot{q}_{ref} - a_n\Lambda e - a_n\lambda\sigma - \eta_2\,\text{sgn}(\sigma). \tag{45}$$

Implementation of the control law (45) is presented in Fig. 2. It consists of the feed-forward control vector $\tau_{ff} = a_n\ddot{q}_{ref} + b_n\dot{q}_{ref}$ to improve transient performances, the feedback control vector $\tau_{fb} = -a_n\Lambda e$ to enhance stability, the disturbance compensation vector $\hat{\tau}_{dis} = -a_n\lambda\sigma$ to attenuate the generalized disturbance vector τ_{dis}, and the sliding control vector $\tau_v = -\eta_2\text{sgn}(\sigma)$ to provide robustness to the disturbance compensation error vector p.

IV. Simulation and Experimental Results

Simulations and experiments are based on the small-scale helicopter system CE 150. Although various reference signals were tested, the step inputs are presented here, due to the performance comparison with the previous control algorithms [12]–[14], which are already implemented to the helicopter system CE 150 and reported the most promising tracking performance. The reference inputs are simultaneously changed in all conducted simulations and experiments, with the smoothed steps due to the nominal control that includes the reference derivative. Here, the controller parameters are not tuned for the best performance, but rather to illustrate robustness properties of the proposed control scheme to the internal and external disturbances. All results are presented for the following values of the controller parameters: $\Lambda = \text{diag}(4, 6)$, $\lambda = \text{diag}(0.4, 0.7)$ and $\eta_2 = 5$.

A. Simulation results

According to the Section II and Section III, the simulation model of the helicopter system CE 150 and the proposed control method were developed using MATLAB. In the simulation mode, 30% uncertainties on the model parameters are included. Furthermore, variable wind disturbances with significantly strong amplitudes (speeds) of $10\,^{\text{m}}/_{\text{s}}$ are represented by the periodic signals with high-frequency $50\,^{\text{rad}}/_{\text{s}}$ and the low-frequency $0.5\,^{\text{rad}}/_{\text{s}}$, which are added to both, the elevation and azimuth dynamics in order to represent wind gusts. The elevation and azimuth tracking errors of the RIC based SMC scheme and the DOB based SMC algorithm [13] are compared and presented in Fig. 3 and Fig. 4. It can be noticed that RIC based SMC structure stabilized the closed-loop system and maintained the helicopter attitude over the whole domain, even in the presence of additional external and internal disturbances. In comparison with the DOB based SMC, the proposed method obtained superior tracking performances, with lower overshoots and steady state errors.

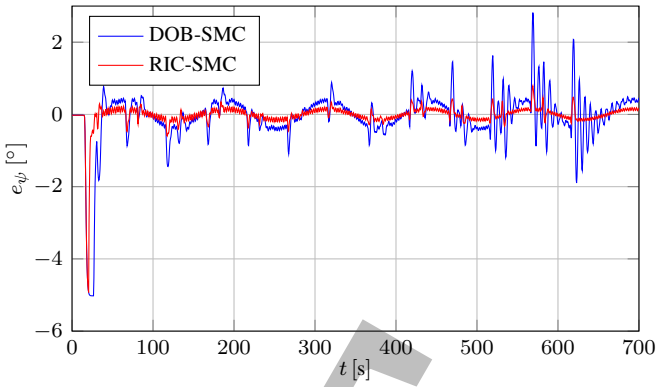

Fig. 3: Comparison of the elevation tracking errors in the sim. mode

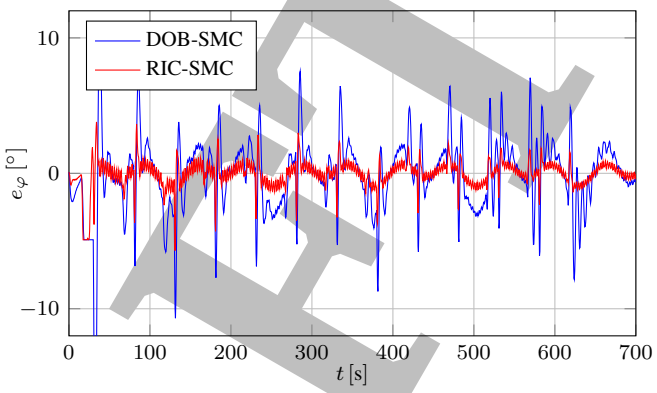

Fig. 4: Comparison of the azimuth tracking errors in the sim. mode

B. Experimental results

In this subsection the perturbation test is demonstrated at the real helicopter system CE 150 to investigate tracking performance of the developed control scheme and its robustness to additional disturbances. The perturbation test is applied by the ballast movement along its horizontal axis, thus simulating dynamical changes in the center of gravity. At the beginning of the test, the ballast is at the default position, that is the middle of the axis. About 150 second of the test, the ballast motion is started from the start point to the end point of the horizontal axis using the third control input. The test

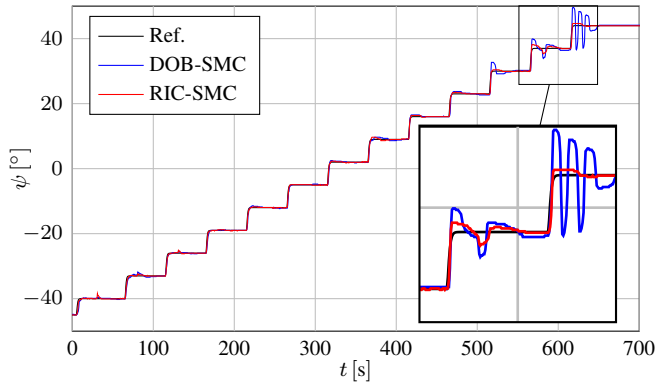

Fig. 5: Comparison of the elevation angle responses at the real exp.

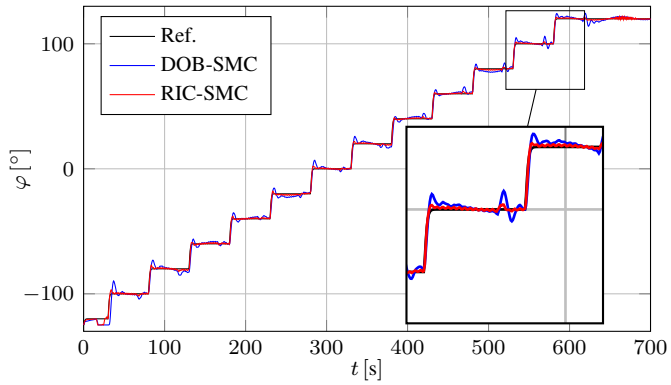

Fig. 6: Comparison of the azimuth angle responses at the real exp.

results are presented in Fig. 5 and Fig. 6. In comparison with the DOB based SMC method, the RIC based SMC algorithm exhibited improved tracking performances under the perturbation test, with lower overshoots and steady state errors, especially when the elevation and the azimuth angle limits are approached.

V. Conclusions

In this paper the synthesis of the I-SMC and the RIC is proposed for a class of nonlinear uncertain MIMO systems. This represents a generalisation of the well-known RIC based control for linear SISO systems, providing a more elegant solution than trying to utilize a decouple set of single variable control schemes. The designed control algorithm is implemented to the highly nonlinear small-scale helicopter system CE 150. It has demonstrated an excellent attitude tracking performance and robust stability in the presence of uncertainties due to model simplifications, parameter variations, strong cross-couplings and unknown dynamics. Numerical simulations and real experiments have approved the robustness of the developed control structure even to the additional disturbances which have been added to the system in the form of wind gusts with high amplitudes, 30% uncertainties on the model parameters, and ballast displacements during flight tests.

References

[1] V. I. Utkin, *Sliding modes in control and optimization*. Springer-Verlag, 1992.

[2] A. J. Healey and D. Lienard, "Multivariable sliding mode control for autonomous diving and steering of unmanned underwater vehicles," *Oceanic Engineering, IEEE Journal of*, vol. 18, no. 3, pp. 327–339, 1993.

[3] K. D. Young, V. I. Utkin, and U. Ozguner, "A control engineer's guide to sliding mode control," *IEEE transactions on control systems technology*, vol. 7, no. 3, pp. 328–342, 1999.

[4] J. P. V. Cunha, L. Hsu, R. R. Costa, and F. Lizarralde, "Output-feedback model-reference sliding mode control of uncertain multivariable systems," *Automatic Control, IEEE Transactions on*, vol. 48, no. 12, pp. 2245–2250, 2003.

[5] A. Pisano and E. Usai, "Sliding mode control: A survey with applications in math," *Mathematics and Computers in Simulation*, vol. 81, no. 5, pp. 954–979, 2011.

[6] I. Nagesh and C. Edwards, "A multivariable super-twisting sliding mode approach," *Automatica*, vol. 50, no. 3, pp. 984–988, 2014.

[7] B. K. Kim and W. K. Chung, "Performance predictable design of robust motion controllers for high-precision servo systems," in *American Control Conference, 2001. Proceedings of the 2001*, vol. 3, 2001, pp. 2249–2254 vol.3.

[8] ——, "Unified analysis and design of robust disturbance attenuation algorithms using inherent structural equivalence," in *American Control Conference, 2001. Proceedings of the 2001*, vol. 5, 2001, pp. 4046–4051 vol.5.

[9] ——, "Advanced design of disturbance observer for high performance motion control systems," in *American Control Conference, 2002. Proceedings of the 2002*, vol. 3, 2002, pp. 2112–2117.

[10] ——, "Performance tuning of robust motion controllers for high-accuracy positioning systems," *Mechatronics, IEEE/ASME Transactions on*, vol. 7, no. 4, pp. 500–514, Dec 2002.

[11] B. K. Kim, W. K. Chung, and K. Ohba, "Design and performance tuning of sliding-mode controller for high-speed and high-accuracy positioning systems in disturbance observer framework," *Industrial Electronics, IEEE Transactions on*, vol. 56, no. 10, pp. 3798–3809, Oct 2009.

[12] A. Salihbegovic, E. Sokic, N. Osmic, and M. Hebibovic, "High performance disturbance observer based control of the nonlinear 2dof helicopter system," in *Information, Communication and Automation Technologies (ICAT), 2013 XXIV International Symposium on*, 2013, pp. 1–7.

[13] A. Salihbegovic and M. Hebibovic, "Attitude tracking of the small-scale helicopter system using disturbance observer based sliding mode control," in *Control and Automation (MED), 2014 22nd Mediterranean Conference of*, June 2014, pp. 1578–1583.

[14] J. Velagic and N. Osmic, "Fuzzy-genetic identification and control stuctures for nonlinear helicopter model," *Intelligent Automation & Soft Computing*, vol. 19, no. 1, pp. 51–68, 2013.

[15] J. Balderud and D. I. Wilson, "A comparison of optimal control strategies for a toy helicopter," in *Asian Control Conference*, Singapore, Sep 2002, pp. 1432 – 1437.

[16] A. Šabanović and K. Ohnishi, *Motion control systems*. Chichester, United Kingdom: Wiley & Sons, Ltd, 2011.

[17] H. Khalil, *Nonlinear Systems*. Prentice Hall, Jan. 2002.

[18] A. Salihbegovic, M. Hebibovic, and E. Sokic, "Synthesis of the integral sliding mode control and the robust internal-loop compensator for a class of nonlinear systems with matched uncertainties," in *Information, Communication and Automation Technologies (ICAT), 2015 XXV International Conference on*, Oct 2015, pp. 1–8.